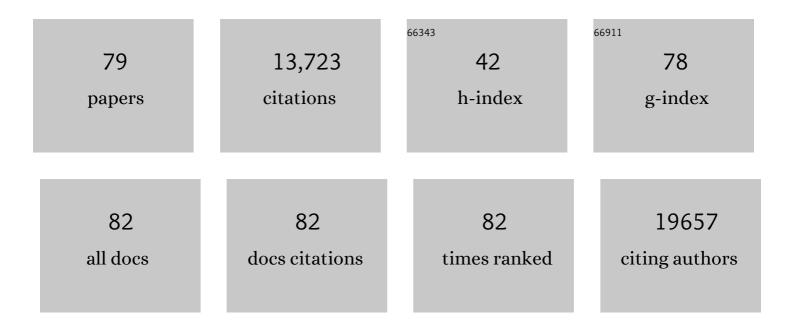
## Lehui Lu

List of Publications by Year in descending order

Source: https://exaly.com/author-pdf/7823784/publications.pdf Version: 2024-02-01



Lenn Lu

#	Article	IF	CITATIONS
1	Polydopamine and Its Derivative Materials: Synthesis and Promising Applications in Energy, Environmental, and Biomedical Fields. Chemical Reviews, 2014, 114, 5057-5115.	47.7	3,865
2	Dopamineâ€Melanin Colloidal Nanospheres: An Efficient Nearâ€Infrared Photothermal Therapeutic Agent for In Vivo Cancer Therapy. Advanced Materials, 2013, 25, 1353-1359.	21.0	1,688
3	Sp <sup>2</sup> Câ€Dominant Nâ€Doped Carbon Subâ€micrometer Spheres with a Tunable Size: A Versatile Platform for Highly Efficient Oxygenâ€Reduction Catalysts. Advanced Materials, 2013, 25, 998-1003.	21.0	798
4	Magnetite/reduced graphene oxide nanocomposites: One step solvothermal synthesis and use as a novel platform for removal of dye pollutants. Nano Research, 2011, 4, 550-562.	10.4	588
5	A Superhydrophobic Sponge with Excellent Absorbency and Flame Retardancy. Angewandte Chemie - International Edition, 2014, 53, 5556-5560.	13.8	428
6	Comprehensive Insights into the Multi-Antioxidative Mechanisms of Melanin Nanoparticles and Their Application To Protect Brain from Injury in Ischemic Stroke. Journal of the American Chemical Society, 2017, 139, 856-862.	13.7	404
7	MoS <sub>2</sub> Nanosheets with Widened Interlayer Spacing for Highâ€Efficiency Removal of Mercury in Aquatic Systems. Advanced Functional Materials, 2016, 26, 5542-5549.	14.9	362
8	Highâ€Rate Oxygen Electroreduction over Graphiticâ€N Species Exposed on 3D Hierarchically Porous Nitrogenâ€Doped Carbons. Angewandte Chemie - International Edition, 2014, 53, 9503-9507.	13.8	355
9	Largeâ€Area Silverâ€Coated Silicon Nanowire Arrays for Molecular Sensing Using Surfaceâ€Enhanced Raman Spectroscopy. Advanced Functional Materials, 2008, 18, 2348-2355.	14.9	354
10	A Highâ€Performance Ytterbiumâ€Based Nanoparticulate Contrast Agent for Inâ€Vivo Xâ€Ray Computed Tomography Imaging. Angewandte Chemie - International Edition, 2012, 51, 1437-1442.	13.8	317
11	Largeâ€Scale Synthesis of Bi <sub>2</sub> S <sub>3</sub> Nanodots as a Contrast Agent for In Vivo Xâ€ray Computed Tomography Imaging. Advanced Materials, 2011, 23, 4886-4891.	21.0	308
12	Targeted polydopamine nanoparticles enable photoacoustic imaging guided chemo-photothermal synergistic therapy of tumor. Acta Biomaterialia, 2017, 47, 124-134.	8.3	216
13	A novel strategy for making soluble reduced graphene oxide sheets cheaply by adopting an endogenous reducing agent. Journal of Materials Chemistry, 2011, 21, 3365-3370.	6.7	208
14	Polydopamine-based coordination nanocomplex for T1/T2 dual mode magnetic resonance imaging-guided chemo-photothermal synergistic therapy. Biomaterials, 2016, 77, 198-206.	11.4	187
15	Seed-mediated growth of large, monodisperse core–shell gold–silver nanoparticles with Ag-like optical properties. Chemical Communications, 2002, , 144-145.	4.1	179
16	Structural effects of a carbon matrix in non-precious metal O <sub>2</sub> -reduction electrocatalysts. Chemical Society Reviews, 2016, 45, 2396-2409.	38.1	175
17	Multifunctional envelope-type mesoporous silica nanoparticles for pH-responsive drug delivery and magnetic resonance imaging. Biomaterials, 2015, 60, 111-120.	11.4	171
18	Preparation, Structure, and Properties of Three-Dimensional Ordered α-Fe2O3Nanoparticulate Film. Chemistry of Materials, 2000, 12, 790-794.	6.7	166

#	Article	IF	CITATIONS
19	Bacteria promoted hierarchical carbon materials for high-performance supercapacitor. Energy and Environmental Science, 2012, 5, 6206.	30.8	163
20	Controlled Fabrication of Gold-Coated 3D Ordered Colloidal Crystal Films and Their Application in Surface-Enhanced Raman Spectroscopy. Chemistry of Materials, 2005, 17, 5731-5736.	6.7	147
21	Defect Engineering Enables Synergistic Action of Enzyme-Mimicking Active Centers for High-Efficiency Tumor Therapy. Journal of the American Chemical Society, 2021, 143, 8855-8865.	13.7	146
22	Transition metal–nitrogen–carbon nanostructured catalysts for the oxygen reduction reaction: From mechanistic insights to structural optimization. Nano Research, 2017, 10, 1449-1470.	10.4	144
23	Ordered Macroporous Bimetallic Nanostructures: Design, Characterization, and Applications. Accounts of Chemical Research, 2008, 41, 244-253.	15.6	143
24	Fabrication of core-shell Au-Pt nanoparticle film and its potential application as catalysis and SERS substrateElectronic supplementary information (ESI) available: AFM image and line scans of core-shell Au-Pt nanoparticle film (colour version of Fig. 4). See http://www.rsc.org/suppdata/jm/b3/b314868h/. Journal of Materials Chemistry, 2004, 14, 1005.	6.7	141
25	Plasmonic titanium nitride nanoparticles for inÂvivo photoacoustic tomography imaging and photothermal cancer therapy. Biomaterials, 2017, 132, 37-47.	11.4	136
26	Monitoring catalytic degradation of dye molecules on silver-coated ZnO nanowire arrays by surface-enhanced Raman spectroscopy. Journal of Materials Chemistry, 2009, 19, 5547.	6.7	129
27	Environmentally Friendly Synthesis of Highly Monodisperse Biocompatible Gold Nanoparticles with Urchin-like Shape. Langmuir, 2008, 24, 1058-1063.	3.5	120
28	Biomass-derived carbon materials for high-performance supercapacitor electrodes. RSC Advances, 2014, 4, 30887.	3.6	95
29	Glycyl Glycine Templating Synthesis of Single-Crystal Silver Nanoplates. Crystal Growth and Design, 2006, 6, 2155-2158.	3.0	70
30	Improved size control of large palladium nanoparticles by a seeding growth method. Journal of Materials Chemistry, 2002, 12, 156-158.	6.7	69
31	A Superhydrophobic Sponge with Excellent Absorbency and Flame Retardancy. Angewandte Chemie, 2014, 126, 5662-5666.	2.0	69
32	Inorganic layered ion-exchangers for decontamination of toxic metal ions in aquatic systems. Journal of Materials Chemistry A, 2017, 5, 19593-19606.	10.3	68
33	Flame-retardant porous hexagonal boron nitride for safe and effective radioactive iodine capture. Journal of Materials Chemistry A, 2019, 7, 16850-16858.	10.3	66
34	A C <sub>5</sub> N <sub>2</sub> Nanoparticle Based Direct Nucleus Delivery Platform for Synergistic Cancer Therapy. Angewandte Chemie - International Edition, 2019, 58, 6290-6294.	13.8	63
35	Multiplex electrochemiluminescence DNA sensor for determination of hepatitis B virus and hepatitis C virus based on multicolor quantum dots and Au nanoparticles. Analytica Chimica Acta, 2016, 916, 92-101.	5.4	62
36	Facile preparation and performance of mesoporous manganese oxide for supercapacitors utilizing neutral aqueous electrolytes. RSC Advances, 2012, 2, 3298.	3.6	61

#	Article	IF	CITATIONS
37	An ultrasmall and metabolizable PEGylated NaGdF <sub>4</sub> :Dy nanoprobe for high-performance T <sub>1</sub> /T <sub>2</sub> -weighted MR and CT multimodal imaging. Nanoscale, 2015, 7, 15680-15688.	5.6	58
38	Synergistic Tailoring of Electrostatic and Hydrophobic Interactions for Rapid and Specific Recognition of Lysophosphatidic Acid, an Early-Stage Ovarian Cancer Biomarker. Journal of the American Chemical Society, 2017, 139, 11616-11621.	13.7	58
39	Wearable and Biodegradable Sensors for Human Health Monitoring. ACS Applied Bio Materials, 2021, 4, 122-139.	4.6	52
40	Targeted Engineering of Medicinal Chemistry for Cancer Therapy: Recent Advances and Perspectives. Angewandte Chemie - International Edition, 2021, 60, 5626-5643.	13.8	47
41	Multi-positively charged dendrimeric nanoparticles induced fluorescence quenching of graphene quantum dots for heparin and chondroitin sulfate detection. Biosensors and Bioelectronics, 2015, 74, 284-290.	10.1	45
42	Host-guest interaction-mediated nanointerface engineering for radioiodine capture. Nano Today, 2021, 36, 101034.	11.9	45
43	Nanoparticulate X-ray CT contrast agents. Science China Chemistry, 2015, 58, 753-760.	8.2	43
44	Hydrogen bond-mediated strong adsorbent–I <sub>3</sub> <sup>â^'</sup> interactions enable high-efficiency radioiodine capture. Materials Horizons, 2019, 6, 1517-1525.	12.2	43
45	An enhanced electrochemical platform based on graphene-polyoxometalate nanomaterials for sensitive determination of diphenolic compounds. Analytical Methods, 2011, 3, 1587.	2.7	42
46	Revisiting the Structure of Graphene Oxide for Preparing Newâ€Style Grapheneâ€Based Ultraviolet Absorbers. Advanced Functional Materials, 2012, 22, 2542-2549.	14.9	41
47	Achieving ultrasensitive inÂvivo detection of bone crack with polydopamine-capsulated surface-enhanced Raman nanoparticle. Biomaterials, 2017, 114, 54-61.	11.4	40
48	An Allâ€inâ€One Organic Semiconductor for Targeted Photoxidation Catalysis in Hypoxic Tumor. Angewandte Chemie - International Edition, 2021, 60, 16641-16648.	13.8	36
49	Targeted Imaging of Damaged Bone <i>in Vivo</i> with Gemstone Spectral Computed Tomography. ACS Nano, 2016, 10, 4164-4172.	14.6	35
50	Si-assisted N, P Co-doped room temperature phosphorescent carbonized polymer Dots: Information Encryption, graphic Anti-counterfeiting and biological imaging. Journal of Colloid and Interface Science, 2022, 609, 279-288.	9.4	35
51	A novel aptamer-mediated CuInS <sub>2</sub> quantum dots@graphene oxide nanocomposites-based fluorescence "turn off–on―nanosensor for highly sensitive and selective detection of kanamycin. RSC Advances, 2016, 6, 10205-10214.	3.6	30
52	A new type of nanoscale coordination particles: toward modification-free detection of hydrogen sulfide gas. Journal of Materials Chemistry, 2012, 22, 18418.	6.7	24
53	A Versatile and Scalable Approach toward Robust Superhydrophobic Porous Materials with Excellent Absorbency and Flame Retardancy. Scientific Reports, 2016, 6, 31233.	3.3	23
54	CO <sub>2</sub> -based amphiphilic polycarbonate micelles enable a reliable and efficient platform for tumor imaging. Theranostics, 2017, 7, 4689-4698.	10.0	23

#	Article	IF	CITATIONS
55	Direct monitoring of trace water in Li-ion batteries using <i>operando</i> fluorescence spectroscopy. Chemical Science, 2018, 9, 231-237.	7.4	22
56	Nanoscaled porphyrinic metal–organic framework for photodynamic/photothermal therapy of tumor. Electrophoresis, 2019, 40, 2204-2210.	2.4	22
57	Cotton-assisted preparation of mesoporous manganese oxide for supercapacitors. RSC Advances, 2012, 2, 6741.	3.6	20
58	Porous β-cyclodextrin nanotubular assemblies enable high-efficiency removal of bisphenol micropollutants from aquatic systems. Nano Research, 2020, 13, 1933-1942.	10.4	20
59	In situ synthesis of monodisperse luminescent terbium complex-silica nanocomposites. Journal of Materials Chemistry, 2004, 14, 2760.	6.7	19
60	Delineating the tumor margin with intraoperative surface-enhanced Raman spectroscopy. Analytical and Bioanalytical Chemistry, 2019, 411, 3993-4006.	3.7	19
61	Polypyrrole-based double rare earth hybrid nanoparticles for multimodal imaging and photothermal therapy. Journal of Materials Chemistry B, 2020, 8, 426-437.	5.8	18
62	Selective Crystallization of BaF2 under a Compressed Langmuir Monolayer of Behenic Acid. Chemistry of Materials, 2001, 13, 325-328.	6.7	16
63	Mitochondria-Targeting Enhanced Phototherapy by Intrinsic Characteristics Engineered "One-for-All― Nanoparticles. ACS Applied Materials & Interfaces, 2021, 13, 35568-35578.	8.0	16
64	Point-and-Shoot Strategy for Identification of Alcoholic Beverages. Analytical Chemistry, 2018, 90, 9838-9844.	6.5	14
65	A C 5 N 2 Nanoparticle Based Direct Nucleus Delivery Platform for Synergistic Cancer Therapy. Angewandte Chemie, 2019, 131, 6356-6360.	2.0	12
66	On-demand degradable magnetic resonance imaging nanoprobes. Science Bulletin, 2021, 66, 676-684.	9.0	12
67	Metal-Phenolic Encapsulated Mesoporous Silica Nanoparticles for pH-Responsive Drug Delivery and Magnetic Resonance Imaging. Zeitschrift Fur Physikalische Chemie, 2018, 232, 1733-1740.	2.8	11
68	Unveiling the Role of Hydroxyl Architecture on Polysulfide Trapping for High-Performance Lithium–Sulfur Batteries. ACS Applied Energy Materials, 2020, 3, 4023-4032.	5.1	11
69	An Allâ€inâ€One Organic Semiconductor for Targeted Photoxidation Catalysis in Hypoxic Tumor. Angewandte Chemie, 2021, 133, 16777-16784.	2.0	9
70	Dual-responsive nano-prodrug micelles for MRI-guided tumor PDT and immune synergistic therapy. Journal of Materials Chemistry B, 2022, 10, 4261-4273.	5.8	9
71	Nanoparticles: Untying the Gordian Knot in Conventional Computed Tomography Imaging. CCS Chemistry, 2021, 3, 1242-1257.	7.8	5
72	Molecular construction of oriented crystalline NaMnF3 and KMnF3 with perovskite structures at room temperature. Journal of Colloid and Interface Science, 2003, 266, 115-119.	9.4	4

#	Article	IF	CITATIONS
73	Zielgerichtete Wirkstoffe für die Krebstherapie: Aktuelle Entwicklungen und Perspektiven. Angewandte Chemie, 2021, 133, 5686-5705.	2.0	3
74	Hierarchically porous polymers with ultra-high affinity for bisphenol A enables high efficient water purification. Science China Chemistry, 2021, 64, 1389-1400.	8.2	3
75	Bioinspired nanostructured spiderweb for high-efficiency capturing and killing of bacteria. Science China Materials, 2022, 65, 518-526.	6.3	2
76	Organic template-directed crystallization of the complex fluoride NH4MnF3 with perovskite structure. Chemical Communications, 2001, , 1342-1343.	4.1	1
77	Self-organization of BaF2Single Crystal Film under a Compressed Langmuir Monolayer. Molecular Crystals and Liquid Crystals, 2001, 371, 45-48.	0.3	0
78	New researches of State Key Laboratories in Analytical Chemistry. Science China Chemistry, 2016, 59, 781-782.	8.2	0
79	Imaging Probes Offer New Opportunities for Understanding Cancer. Journal of Analysis and Testing, 2018. 2. 1-1.	5.1	0